JOURNAL OF GEOPHYSICAL RESEARCH, VOL. 113, E09002, doi:10.1029/2007JE003066, 2008

Fractal properties of isolines at varying altitude revealing different dominant geological processes on Earth

Andrea Baldassarri,[1] Marco Montuori,[2] Olga Prieto-Ballesteros,[3] and Susanna C. Manrubia[3]

Received 12 December 2007; revised 2 July 2008; accepted 16 July 2008; published 5 September 2008.

[1] Geometrical properties of landscapes result from the geological processes that have acted through time. The quantitative analysis of natural relief represents an objective form of aiding in the visual interpretation of landscapes, as studies on coastlines, river networks, and global topography, have shown. Still, an open question is whether a clear relationship between the quantitative properties of landscapes and the dominant geomorphologic processes that originate them can be established. In this contribution, we show that the geometry of topographic isolines is an appropriate observable to help disentangle such a relationship. A fractal analysis of terrestrial isolines yields a clear identification of trenches and abyssal plains, differentiates oceanic ridges from continental slopes and platforms, localizes coastlines and river systems, and isolates areas at high elevation (or latitude) subjected to the erosive action of ice. The study of the geometrical properties of the lunar landscape supports the existence of a correspondence between principal geomorphic processes and landforms. Our analysis can be easily applied to other planetary bodies.

Citation: Baldassarri, A., M. Montuori, O. Prieto-Ballesteros, and S. C. Manrubia (2008), Fractal properties of isolines at varying altitude revealing different dominant geological processes on Earth, *J. Geophys. Res.*, *113*, E09002, doi:10.1029/2007JE003066.

1. Introduction

[2] There exists an overwhelming diversity of landscapes on Earth. A cornerstone of modern geomorphology came with the realization that all the different features of the terrestrial surface result from the accumulated effect of current geological agents [*Lyell*, 1830]. This principle established for the first time a qualitative relationship between pattern and process in geology. More than a century later, with the application of fractal geometry to natural systems, the characteristic, rough shapes exhibited by landscapes were identified in a first approximation as self-similar, triggering in this way the research on mechanistic and theoretical models aimed at identifying the underlying constructive rules responsible for the appearance of scale-invariant patterns. Computational analysis of the geometry of coastlines [*Mandelbrot*, 1967, 1983; *Boffetta et al.*, 2008] and river networks [*Mandelbrot*, 1967; *Hack*, 1957; *Rinaldo et al.*, 1993; *Rodríguez-Iturbe and Rinaldo*, 1997; *Niemann et al.*, 2001] placed them among the first natural systems quantitatively characterized. The fact that both systems display quasi-universal properties prompted the search for simple models able to account for their quantitative features. The topology of river networks seems to stem from a principle of transport optimization [*Maritan et al.*, 1996] while the dominant 4/3 fractal dimension of coasts can be retrieved from a damping erosion model [*Sapoval et al.*, 2004]. In comparison, global topography has received less attention, maybe reflecting that at odds with coastlines and rivers, terrestrial topography possesses a more complex scale invariance (is multifractal [*Gagnon et al.*, 2006]) and its geometry depends on specific features of the region analyzed [*Dodds and Rothman*, 2000; *Ivanov*, 1994; *Gagnon et al.*, 2003]. In all cases, fractal geometry has proven useful in the description of natural landscapes because of the characteristic and ubiquitous repetition of similar motifs at different spatial scales. At present, one of the goals of topography analysis is to single out characteristic features with well-defined, scale-invariant properties (in the sense used above for river networks or coasts) as a first step toward distinguishing dominant physical process and the subsequent design of simple models able to reproduce the average geometrical properties of that region.

[3] This ambitious goal is limited by our understanding of the complex feedback loop between the action of geological processes and the surface features of Earth. Geological agents settle the characteristics of the topography but act, in turn, with different strength as a function of elevation [*Weissel et al.*, 1994], the latter being a variable itself on geological timescales. Two clear examples of this interrelationship are coastlines and young mountains. The former are mainly shaped through water erosion and can only occur at the contacts among oceans, emerged lands, and atmosphere. The characteristics of young, high mountains result from orogenic processes and the action of liquid and solid water. Differentiation between lowlands and highlands, where altitude is correlated with geomorphic features,

[1] Dipartimento di Fisica, Università di Roma "La Sapienza," Rome, Italy.
[2] CNR-INFM, Rome, Italy.
[3] Centro de Astrobiología, CSIC-INTA, Madrid, Spain.

0148-0227/08/2007JE003066$09.00

occurs in other planetary bodies as well. Mars is divided into cratered highlands covering most of the southern hemisphere and resurfaced lowlands in the northern hemisphere [*Aharonson et al.*, 2001]. The surface of Venus can be divided, in its turn, into the following three main regions according to elevation: highlands characterized by volcanic and strongly tectonized structures, mesolands dominated by large extensional fracture belts and several volcanic features, and lowlands mainly shaped through volcanism [*Bazilevski et al.*, 1982; *Price and Suppe*, 1995]. Taking into account the clear differentiation in morphological structures as a function of their elevation, an analysis of the global topography based on measures that mix several heights could jumble different features. Hence, the use of isolines, defined as the set of points at a fixed elevation, appears as a suitable solution to undertake a quantification of topography [*Isichenko*, 1992; *Kondev et al.*, 2000]. The fractal dimension D, a measure of the degree of self-similarity of a curve, will be used to characterize in a first approximation the geometrical properties of isolines.

[4] At present, comparative geomorphology is the everyday tool used by geologists to infer the geological processes responsible for the structures observed not only on Earth but on any planetary body. This qualitative analysis of classical geomorphology can experience a boost with the use of technical advances yielding direct and precise measurements of topographic relief. An accurate and objective quantification of such data is of prime relevance to identify major geological processes on Earth and elsewhere [*Dodds and Rothman*, 2000; *Ivanov*, 1994; *Gagnon et al.*, 2006; *Maritan et al.*, 1996; *Turcotte*, 1997; *Wilson and Dominic*, 1998; *Sung and Chen*, 2004]. In this work, we take advantage of the large amount of topographic data available to obtain reliable, three-dimensional models of planetary surfaces. At present, the Earth, the Moon, and Mars are well characterized, so their global topography is susceptible to being quantitatively studied. Our aim is to introduce a formal methodology that represents a first step toward the unsupervised identification of major topographic characteristics of landscapes. The method we propose is based on the measure of the local fractal dimension of isolines on the whole planetary surface. A statistical analysis of the results advances in establishing a correspondence between topographic features and intervening geological agents.

2. Isoline Analysis

[5] Topographic data for Earth have been obtained from the SRTM30plus data set. The data consist of measured elevations over a grid of surface points. The resolution is of 30" (approximately 1 km) for continental land, and of 2' (approximately 4 km) for seafloor topography (SRTM data are available at http://topex.ucsd.edu/WWW_html/srtm30_plus.html). Topographic data for the Moon come from the Clementine project [*Nozette et al.*, 1994; Clementine data are available at http://nssdc.gsfc.nasa.gov/planetary/clementine.html] and have a resolution of 30'. Our analysis will be restricted to the lunar region spanning 70°S to 70°N since direct measures of altimetry from the Clementine project covered approximately that band [*Smith et al.*, 1997].

[6] Isolines for both bodies have been identified at intervals of 100 m. To determine the points belonging to an isoline at level h, we select pairs of neighboring measures in the grid with positions p_1 and p_2 and corresponding elevations h_1 and h_2, with the condition that $h_1 \geq h \geq h_2$. We assayed the following three different definitions of isolines: (1) both p_1 and p_2 belong to the isoline at level h; (2) only p_2 (compare p_1) belongs to the isoline; and (3) a single isolated point with averaged position (coordinates) between p_1 and p_2 belongs to the isoline. Either definition yielded exactly the same quantitative results. An isoline is finally a set of N points, with N not larger than the number of measures in the original, finite data set. This procedure is analogous to the functional box counting introduced in previous studies [e.g., *Lovejoy and Schertzer*, 1991].

[7] We have computed the fractal dimension of each isoline through the usual box-counting method using square boxes of linear size r and calculating at each scale the number of boxes needed to cover all of the points in the isoline. The isolines we are measuring are not fractal objects in a strict mathematical sense. The spatial scale of potential self-similarity is bound from below by the resolution of the available data and from above by the requirement of analyzing a geologically homogeneous region. Data become too sparse at small scales, such that in practice there are more empty small boxes that would be found if the isoline could be described with arbitrarily small resolution. This causes a bending toward lower fractal dimensions (slope zero is reached below the grid size, when the number of full boxes becomes independent of scale). Further, we are carrying out a systematic, unsupervised analysis of a huge data set. This constrains the range by demanding a minimum and maximum linear scale valid for all situations. Eventually, interpolation to obtain the fractal dimension will be performed within a conservative range ($r_{\min}$, $r_{\max}$) with $r_{\min}$ of the order of few kilometers and $r_{\max}$ around several tens of kilometers. As an example, in the terrestrial region between 60°S and 60°N, we work in angular coordinates corresponding to $r_{\min} = 0.06°$ and $r_{\max} = 0.6°$ (at terrestrial equator, 1° longitude spans about 111 km). Similarly, for the Moon we use $r_{\min} = 0.5°$ and $r_{\max} = 5.0°$. Measures of the fractal dimension of isolines are performed on a set of angular regions, hereinafter denoted "cells" that fully cover the planetary surface. For the Earth we choose a cell size of 4° latitude × 4° longitude and for the Moon 15° latitude × 15° longitude. Linear size of cells is chosen about 10 times larger than $r_{\max}$, once more in order to avoid size effects (too close to the cell size all boxes are full and the fractal dimension crosses over to value 2). In each cell, we computed the fractal dimension for every isoline present. As a result, we get tens of thousands of measures, each one corresponding to a fractal dimension D(lon,lat,h) where h is the elevation of the portion of isoline contained in the cell centered at longitude lon and latitude lat.

[8] Figure 1 shows the results of box counting performed on six terrestrial cells at different elevations, as shown in the legend. The corresponding cells and isolines are plotted in Figure 6c (two examples at elevation 2000 m are shown, only one of them appears in Figure 6c), where the geographical location is also given. As shown, all isolines are fairly self-similar in the range selected for interpolation (straight lines) and even at larger or smaller scales. The bending at small scales due to insufficient sampling is

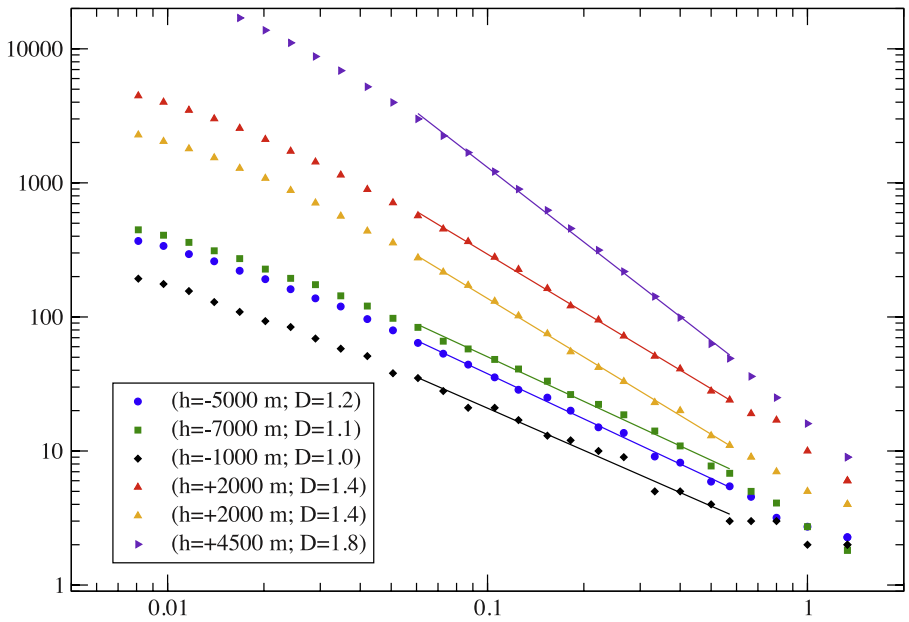

Figure 1. Box-counting results for isolines at different elevations. Straight lines are interpolations on the range used to calculate D. The bending at small scales due to insufficient sampling (not enough points in the isoline close to grid resolution) is seen in all curves as well as the noisy behavior at large scales (not enough boxes as they approach the linear size of the cell). There is a clear variation of D with elevation. See main text for further explanations.

observed in all cases. Finally, there is a clear variation in fractal dimension as a function of elevation.

[9] In our analyses, we have discarded fractal dimensions obtained from isolines with less than $N = 500$ points for the Earth and $N = 200$ points for the Moon. The regression error in the fractal dimension D never exceeded 4%. We tested the robustness of our results by repeating the whole numerical analysis in the following cases: (1) full resolution for continental land ($30''$ instead of $2'$); (2) different minimum number of points per isoline ($N = 100$, 1000, and 2000 for the Earth, and $N = 100$ and 500 for the Moon); (3) pruning of the isolines from local connected "islands" (for instance resulting from peaks of mountains or very small craters that could contribute, in the spatial range considered, as a dust of isolated points systematically affecting the measures); (4) changing the size of the tessellation of the planetary surfaces (cell size up to 60° latitude × 60° longitude) and the value of r_{max} up to 6°. The values of the corresponding measured fractal dimensions are slightly affected quantitatively, but the main results do not change. For instance the curves of average fractal dimensions versus elevations show a vertical global shift by about 0.1, though the presence of a qualitative signal which identifies major features from a statistical viewpoint is robust with respect to the enumerated modifications in the algorithm.

3. Results and Discussion

[10] We begin by analyzing the dependence of the average fractal dimension D with the following three relevant parameters, each corresponding to one major possible direction of anisotropy: longitude, latitude, and elevation. Averages with respect to the other two parameters are performed in each case.

[11] In Figure 2, we summarize the results for the Earth. In order to simplify the notation, we use always D to refer to the fractal dimension irrespective of the parameters that have been averaged. In Figure 2a, we show the behavior of the average fractal dimension versus the longitude. In Figure 2b, the average is plotted as a function of the latitude. In Figure 2c, we plot the average fractal dimension versus the elevation. Figure 3 displays the same measures for the Moon. In all these plots, open circles stand for the average value D. In order to highlight possible deviations in the distribution of fractal dimensions, we plot, as solid lines, the values $D + \sigma$ and $D - \sigma$, where σ is the variance of the measured fractal dimensions. As shown, no systematic variations in the distributions are found. A close inspection of the data reveals that on Earth, the average fractal dimension D is only weakly dependent on longitude (Figure 2a) or latitude (Figure 2b) while it shows a complex dependence on elevation (Figure 2c). In contrast, the average fractal dimension D calculated for the Moon (Figure 3) is always weakly dependent on the three variables. Variations are in all cases less than 0.1 around a low value of the fractal dimension $D \approx 1.2$.

[12] As we have already stated, we hypothesize that geometrical properties of topographical features depend in a direct and quantitative manner on the physical processes that shape them. These processes depend on the physical environment (whether the region is embedded in the atmosphere or in the ocean; whether tectonic processes are acting) and on the climatic characteristics of the region (mainly temperature). None of these features varies (on average) as a function of the longitudinal position of the region, and they are only weakly dependent on latitude: there is a temperature gradient toward the poles and other processes might be affected by the magnetic field of the

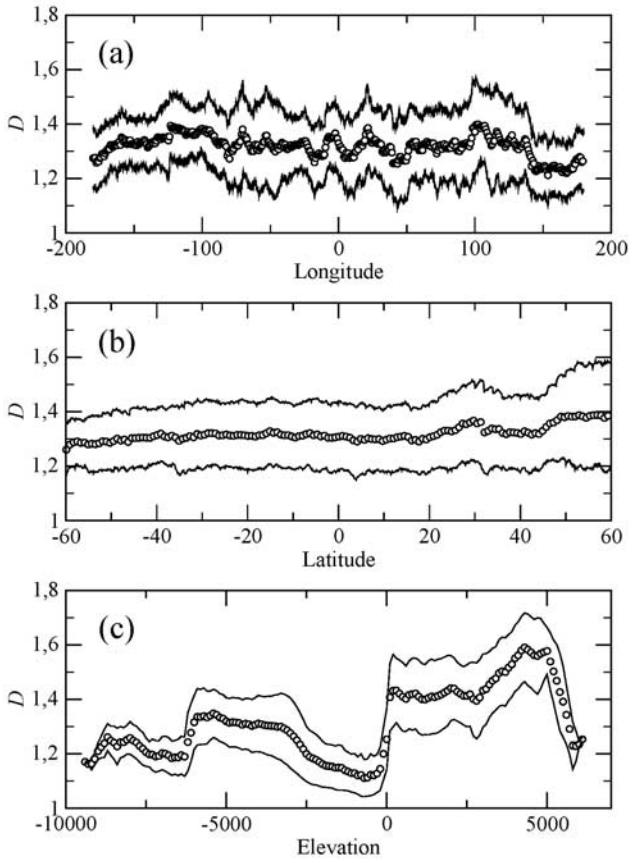

Figure 2. Global average fractal dimension D of terrestrial isolines versus (a) longitude, (b) latitude, and (c) elevation. In each of the plots, D(lon,lat,h) is averaged with respect to two parameters and plotted against the third, as indicated. Circles stand for average values; the statistical error of those measures is smaller than the symbol size. Solid lines represent $D + \sigma$ and $D - \sigma$, where σ is the standard deviation of the distribution of fractal dimensions.

Earth, which breaks the north-south symmetry. However, the fact that the fractal dimension displays average constant values with respect to longitude and latitude reveals that those gradients have at most a mild effect of geomorphology and supports our hypothesis. In contrast, environment changes systematically with elevation, a variable which appears to play a key role in the characterization of large-scale terrestrial morphology.

[13] In Figure 4a, we show a terrestrial world map with the local fractal dimensions of terrestrial isolines. With the purpose of illustrating graphically the qualitative variation of fractal dimension, we have averaged its value over small cells, such that each colored area in the plot corresponds now to a region of 0.1° latitude × 0.1° longitude, its color standing for the average fractal dimension of (isolines contained in) the cell. This procedure amounts to averaging the measures D(lon,lat,h) with respect to a narrow interval of elevations and yields a fractal dimension depending on two parameters, lon and lat (once more, for simplicity, we refer to the measure as D). For comparison, we summarize in Figure 5 the results yielded by performing the same analysis for the lunar surface. Remarkably, and despite the visible difference in cratering between the two longitudinal hemispheres of the Moon, we obtain a distribution of fractal dimensions almost independent of longitude and latitude (see below). It is straightforward to conclude that the large-scale, global topography of the Moon is well described by an average fractal dimension between 1.2 and 1.3. These results give further support to the independence of physical processes with longitude and latitude.

[14] The map depicted in Figure 4a shows several interesting features. Low fractal dimensions (deep blue areas) correspond to smooth regions in oceans, i.e., trenches, continental slopes, and continental platforms. These are either regions with steep slopes (trenches and continental slopes) or smooth areas due to the action of processes such as erosion by water and deposition by marine currents (continental platforms). No regions on continents display such low dimensions, with the exception of areas permanently covered by ice (and because elevation measures are taken on top of ice). Fractal dimensions notably increase along the mid-ocean ridge. Moreover, isoline roughness is higher in regions where transform faults are more abundant (North Atlantic, Indian, and South Pacific oceans). Abyssal floors are to be found between the ridge region and the continental platforms and display a fractal dimension of isolines about 1.3 (dominance of greenish color). Coastlines

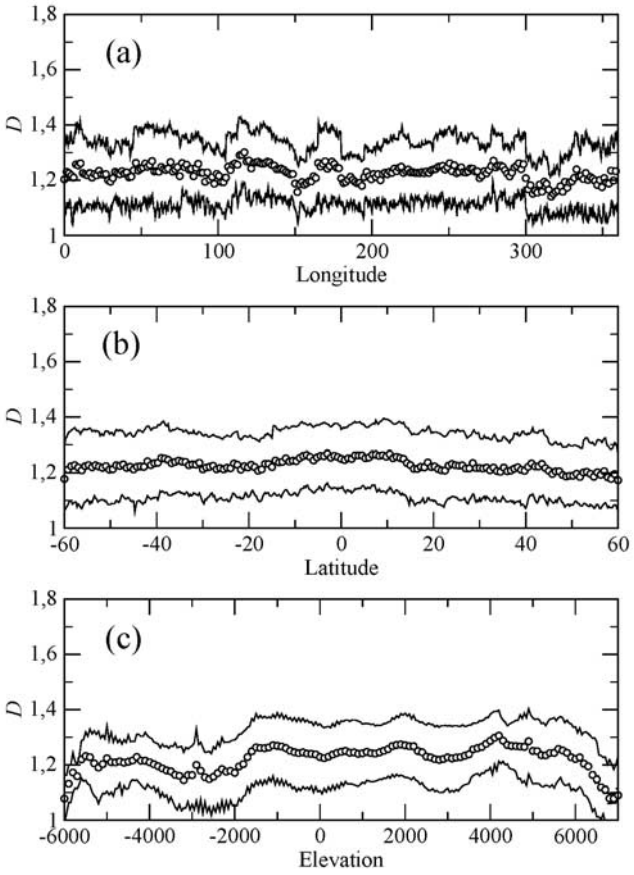

Figure 3. Global average fractal dimension D of lunar isolines versus (a) longitude, (b) latitude, and (c) elevation. Representation as in Figure 2.

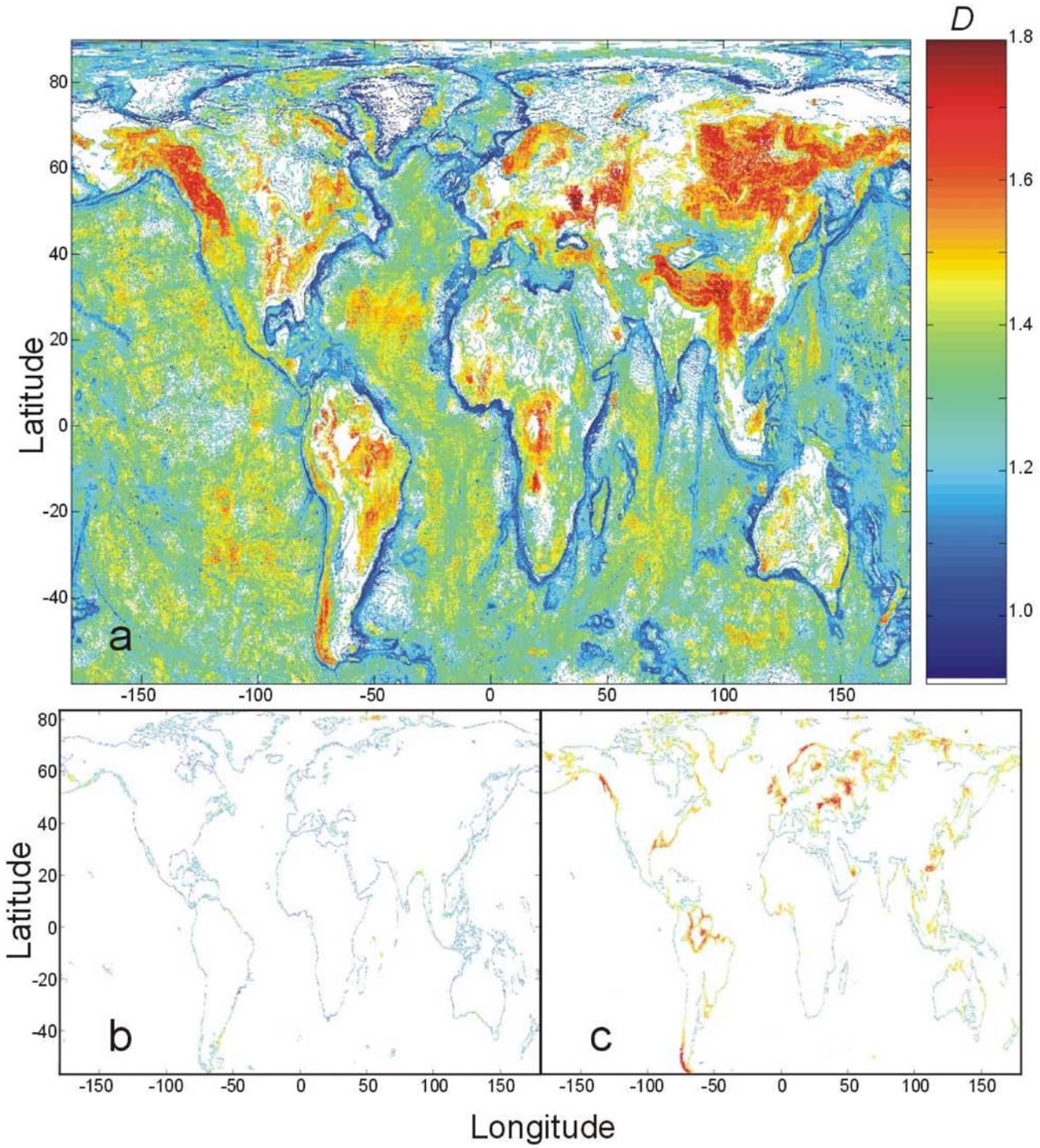

Figure 4. (a) World map representing the local fractal dimensions of isolines. Each point of the map corresponds to a region of 0.1° latitude × 0.1° longitude. The color code indicates the average fractal dimension of isolines within each region. The range of variation of D is broad, from 1.0 to about 1.8. (b) Fractal dimension of isolines at −100 m depth and (c) at 100 m altitude. Below the sea level (Figure 4b), the combined smoothing effects of water erosion and sedimentation yield low fractal dimensions. Figure 4c evidences the dramatic increase in average fractal dimension when coastlines are crossed.

signal the boundary between oceanic and continental regions and are unambiguously identified by our analysis. Figures 4b and 4c display two global isolines; one at 100 m below the sea level and a second one at 100 m elevation on land. Though the profiles of continents are clearly recognized in both cases, the fractal dimension pinpoints a qualitative change in the landscape through a jump from values close to 1.0 below sea level to notably higher values on continental land. In the latter case, a mild dependence of D with latitude along the terrestrial coasts (due to decreases

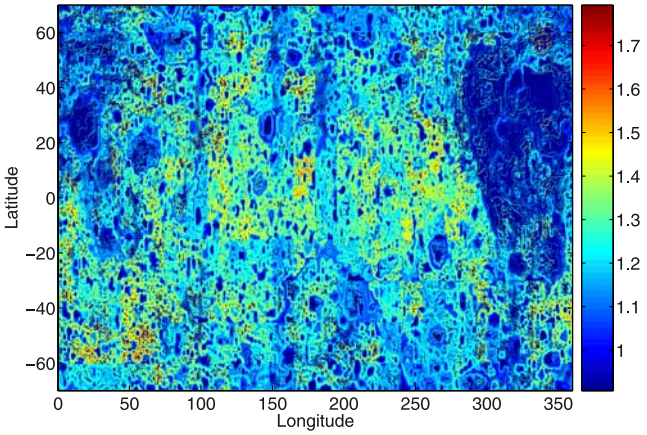

Figure 5. Map of the local fractal dimensions of Moon isolines. A weakly varying fractal dimension, with values between 1.2 and 1.3, speaks for the homogeneity of the lunar surface.

in temperature) is revealed since areas closer to polar regions typically present higher values of D. Continents are even more structured since the effect of latitude and elevation, reflected in strong variations in temperature, is not buffered by the action of oceanic water masses. Furthermore, one expects that water erosion by rivers and ice erosion would increase the complexity of the continental topography.

[15] In order to disentangle the effects of the different processes, we plot in Figure 6a the fractal dimension as a function of latitude and elevation averaged over longitude. First, consider the emerged land, i.e., the right portion of the graph. Here the following two main regions are identified attending to their fractal dimension: (1) a yellow-green band spanning the region from 40°S to 40°N and elevations between ~0 and 2000 m and (2) three patches of high roughness (red color dominant) that correspond, from north to south, to Siberia, to the Himalayan mountains, and to the Andes system (see also Figure 4a).

[16] Regions of high isoline fractal dimensions closely correspond to locations at a high enough latitude or elevation such that ice is conspicuous all through the year. We propose that the cause of such a rough landscape is the strong erosive action of alpine glaciers. In order to support this hypothesis, we have identified a number of places on Earth where the average yearly temperature is about 0°C (±1°C). White symbols in Figure 6a show the position of all those locations: they clearly correlate with the position of isolines with the highest fractal dimension. There are two symbols in the graph. Squares represent actual locations on Earth with yearly average temperature ~0°C. However, not all latitudes have regions with that property, that being because mountains are not high enough at given latitude (as around the equator) or because there are not enough available measures for the location of interest (as in the Andes). In order to fill this gap, we have extrapolated measures taken in locations at the specified latitude but at too low an elevation (hence with average yearly temperatures above 0°C) assuming a decrease of 6°C per 1000 m of increase in elevation. This yields a number of extrapolated data represented as circles (climatic data have been obtained from www.worldclimate.com and www.weatherbase.com).

[17] Above sea level (where the average fractal dimension increases), we identify a range of elevations between 0 and 3000 m at almost constant average fractal dimension: this could correspond to the region spanned by terrestrial river systems. The fact that an almost constant fractal dimension characterizes that region is in agreement with the quasi-universality of the topological properties of river basins and

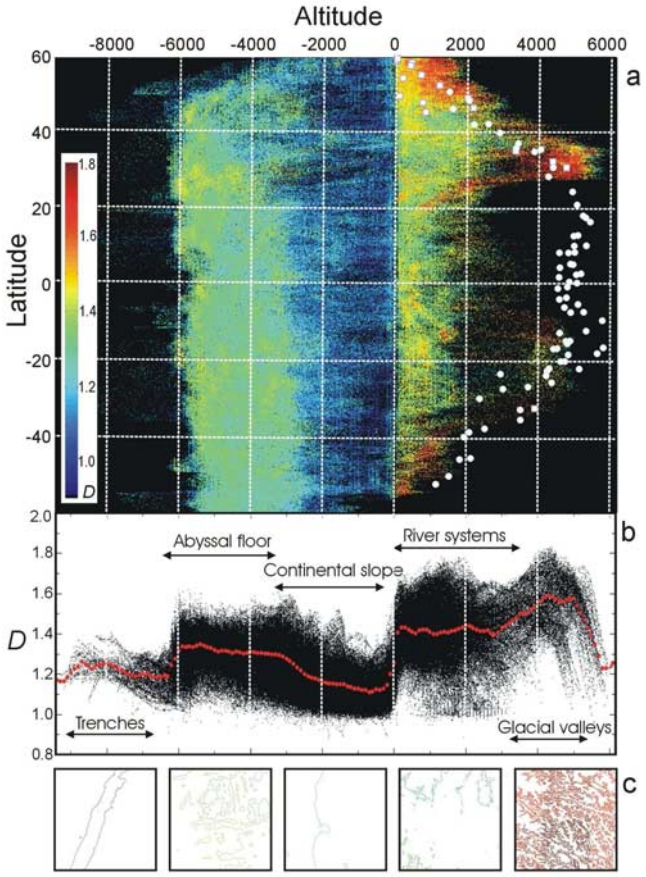

Figure 6. (a) Fractal dimension as a function of latitude and elevation (averaged with respect to longitude). Isolines are measured at intervals of 100 m. White symbols correspond to locations with yearly average temperature about 0°C (see main text). (b) Fractal dimension versus altitude. Black dots correspond to the whole data set represented in color in Figure 6a, while red symbols yield their average value as a function of altitude. This plot contains information equivalent to that in Figure 2c, we include it here for better comparison with Figure 6a. (c) Examples of isolines characterizing major terrestrial geomorphologic features. Each plot covers a surface of 4° latitude × 4° longitude. From left to right, they represent a deep trench (elevation is −7000 m, center of plot is at 32°S, 177°W), the abyssal floor (−5000 m, 18°S, 8°E), a piece of continental slope in the same plate (−1000 m, 18°S, 12°W), a typical continental land dominated by river systems (+2000 m, 32°N, 107°W), and the rough contour of high mountains eroded by ice (+4500 m, 32°N, 97°E).

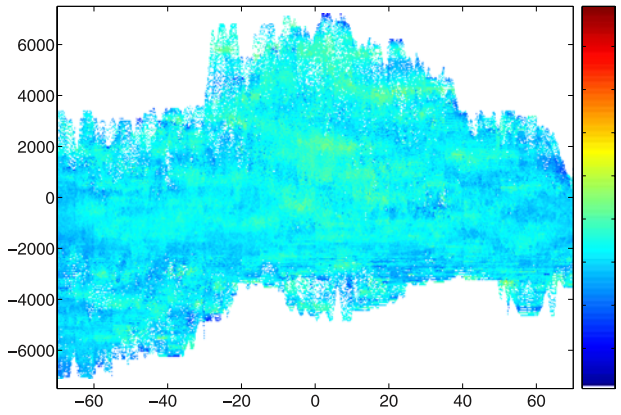

Figure 7. Fractal dimension of Moon isolines as a function of latitude and elevation (averaged with respect to longitude). This is analogous to Figure 6a for Earth.

river networks [*Hack*, 1957; *Caldarelli et al.*, 2004]. Finally, cold regions with glacial valleys are strongly eroded by ice, which we believe to be responsible for the highest average fractal dimensions observed (above 3000 m).

[18] The geometrical properties of regions of the Earth below the sea level (Figure 6a, left) are more weakly dependent on latitude than continents and coasts because of the action of large bodies of water that smooth out temperature variations and maintain a more homogeneous environment. In Figure 6b, we plot the fractal dimension as a function of altitude only, i.e., averaged over latitude and longitude. There we see that ocean basins are divided into three main regions: low-dimensional features at high depths (identified with trenches), rougher structures between −6000 and −3000 m (corresponding to the abyssal floor), and again low-dimensional features between −3000 m and coastlines (this region is dominated by continental slopes). Trenches are narrow topographic depressions caused by the subduction of lithospheric plates, thus characterized by steep slopes and, consequently, rather straight isolines. Abyssal floors are well characterized by a fractal dimension of isolines about 1.3, while continental slopes yield D about 1.1. The continuous increase with depth between regions where those two features dominate is mainly due to the contribution of the mid-ocean ridge, which extends for a length of about 80,000 km with a width of 100 to 4,000 km. Indeed, the ridge significantly contributes to the topographical features in a range spanning −5000 to almost 0 m elevation. Its complex structure systematically heightens the average fractal dimension of isolines as depth increases since the area of the Earth belonging to the ridge province extends with depth. The ocean basin is also decorated with seamounts that contribute at varying depths, mainly from −6000 to −5000 m.

[19] The same analysis for the lunar surface reveals much weaker differences between regions as far as the fractal dimension is concerned (see Figure 7). Actually, while we know a plethora of different agents simultaneously acting on Earth and that tectonism has erased many features from the past, the Moon is a cold, relatively simple planetary body whose surface has only been shaped through meteoritic impacts and the associated lava flows. Two slightly different lunar regions can be identified only after careful inspection of Figure 5 and its comparison with the altimetry obtained from the Clementine project. Several scattered areas with the higher fractal dimensions on the Moon (yellow and orange domains) are found in highlands. These terrains have a rugged relief, with ejecta deposits constituted by large and brecciated rock masses and a plentiful amount of (often superimposed) crater rims. In those regions, the fractal dimension increases locally up to values of 1.4–1.5, but the average stays around 1.3. Lunar lowlands, having experienced similar processes, are nonetheless smoothed out by the lava flows, which have washed out part of the previous relief and cause a decrease in the average fractal dimension to a value around 1.2. This is the region of maria (areas of deep blue in Figure 7), most of them situated on the longitudinal hemisphere facing Earth. The average differences on the Moon are small compared to those measured on the terrestrial surface. Actually, in good agreement with the hypothesis that relates a dominant physical process to an almost constant fractal dimension, a single value of D, weakly dependent on elevation, latitude, or longitude, characterizes the surface of the Moon: the global lunar topography is well described by an average fractal dimension around 1.2 in any region (Figure 3), a narrow interval compared to that of Earth (Figure 2), where remarkably higher values are attained. Taking impact cratering as the initial (and minimal) action that can be suffered by a planetary body, it seems an immediate consequence that any planet with morphological regions characterized by an average fractal dimension above this value had to be shaped by a roughening agent able to increase it. On the contrary, the action of smoothing agents such as lava flows following impacts (as in lunar maria) should work toward further decreasing D.

4. Conclusions

[20] We have presented a statistical analysis of the large-scale morphology of the surface of the Earth and the Moon. Quantification of morphological features has been achieved by measuring the local fractal dimensions of isolines. Variations of the average fractal dimension with different parameters have been considered: on Earth, elevation and occasionally latitude appear as key parameters in order to discriminate different observable features.

[21] A more detailed inspection points to a relation between the observed features and the geological processes that shaped the planetary surface. We suggest that the erosive action of a solid (viscous) phase and the erosion of a flowing liquid phase or its action through wave breaking [*Ashton et al.*, 2001; *Sapoval et al.*, 2004] and tectonics are geological agents which work toward increasing roughness in the landscape. On the other hand, agents causing sediment deposition, formation of pronounced and/or smooth slopes, or erosion through hydrostatic pressure caused by large masses of liquid or ice represent smoothing agents able to decrease the characteristic fractal dimension.

[22] We observe a very complex scenario on Earth according to the broad variation in the local fractal dimension of isolines. These variations correlate to the different specific processes acting in each region. In agreement with our working hypothesis, our analysis identifies a much more

uniform lunar surface where the only shaping processes are impact cratering and lava flows.

[23] Our analysis complements other studies of the scale-invariant properties of terrestrial topology. Studies of the scale invariance of topographic surfaces usually measure correlations in height and perform averages over the horizontal plane [*Gagnon et al.*, 2006]. This procedure washes out angular correlations and cannot yield information on the fractal properties of isolines. It is interesting to remark that both that technique and ours unambiguously establish quantitative differences between continental and oceanic topographies. In *Gagnon et al.* [2006], the parameters characterizing the multifractal properties of continents, oceans, and continental margins were clearly different between those regions but took similar values in separated areas within each of them. Their observations are qualitatively comparable to the acute change in the fractal dimension of isolines that we observe when coasts are crossed. Further, we have observed that oceanic isolines are better represented by monofractals than continental isolines, where bending of the box-counting curve extends over more scales. *Gagnon et al.* [2006] ascribe differences between continents and oceans to qualitatively different processes, remarkably the several sources of erosion acting on continents as opposed to the dominant source of erosion (marine currents) in oceans. This is a possible explanation to the systematic deviation from self-affinity that we observe on continents, though the quantitative characterization of natural topography needs (and deserves) further analysis.

[24] We have shown how the relation between the geometrical properties of isolines and the underlying geomorphologic processes gives clues to undertake a systematic classification of global landscape structures and their geological origin. The method is simple and general enough to be applied to any set of planetary topographic data. For instance, an analogous analysis of Mars morphological data could give insights on the presence of an ancient ocean on that planet.

[25] **Acknowledgments.** The authors acknowledge discussions with J. Chave, F. Colaiori, D. Fernández-Remolar, J. Ormö, J. Pérez-Mercader, B. Sapoval, A. Vulpiani, and S. Zapperi.

References

Aharonson, O., M. T. Zuber, and D. H. Rothman (2001), Statistics of Mars topography from the Mars Orbiter Laser Altimeter: Slopes, correlations, and physical Models, *J. Geophys. Res.*, *106*, 23,723–23,735, doi:10.1029/2000JE001403.

Ashton, A., A. B. Murray, and O. Arnault (2001), Formation of coastline features by large-scale instabilities induced by high-angle waves, *Nature*, *414*, 296–300, doi:10.1038/35104541.

Bazilevski, A. T., N. N. Bobina, V. P. Shashkina, Y. G. Shkuratov, Y. V. Kornienko, A. Y. Usikov, and D. G. Stankevich (1982), On geological processes on Venus: Analysis of the relationship between altitude and degree of surface roughness, *Moon Planets*, *27*, 63–89, doi:10.1007/BF00941558.

Boffetta, G., A. Celani, D. Dezzani, and A. Seminara (2008), How winding is the coast of Britain? Conformal invariance of rocky shorelines, *Geophys. Res. Lett.*, *35*, L03615, doi:10.1029/2007GL033093.

Caldarelli, G., P. De Los Rios, M. Montuori, and V. D. P. Servedio (2004), Statistical features of drainage basins in mars channel networks, *Eur. Phys. J. B*, *38*, 387–391, doi:10.1140/epjb/e2004-00132-y.

Dodds, P. S., and D. H. Rothman (2000), Scaling, universality, and geomorphology, *Annu. Rev. Earth Planet. Sci.*, *28*, 571–610, doi:10.1146/annurev.earth.28.1.571.

Gagnon, J.-S., S. Lovejoy, and D. Schertzer (2003), Multifractal surfaces and terrestrial topography, *Europhys. Lett.*, *62*, 801–807, doi:10.1209/epl/i2003-00443-7.

Gagnon, J.-S., S. Lovejoy, and D. Schertzer (2006), Multifractal earth topography, *Nonlinear Processes Geophys.*, *13*, 541–570.

Hack, T. J. (1957), Submerged river system of Chesapeake Bay, *Geol. Soc. Am. Bull.*, *68*, 817–830, doi:10.1130/0016-7606 (1957)68[817:SRSOCB]2.0.CO;2.

Isichenko, M. B. (1992), Percolation, statistical topography, and transport in random media, *Rev. Mod. Phys.*, *64*, 961–1043, doi:10.1103/RevModPhys.64.961.

Ivanov, S. S. (1994), Estimation of fractal dimension of the global relief, *Oceanology, Engl. Transl.*, *34*, 94–98.

Kondev, J., C. L. Henley, and D. G. Salinas (2000), Nonlinear measures for characterizing rough surface morphologies, *Phys. Rev. E*, *61*, 104–125, doi:10.1103/PhysRevE.61.104.

Lovejoy, S., and D. Schertzer (1991), Multifractal analysis techniques and the rain and cloud fields from 10^{-3} to 10^{6}m, in *Non-linear Variability in Geophysics: Scaling and Fractals*, edited by D. Schertzer and S. Lovejoy, pp. 111–144, Springer, New York.

Lyell, C. (1830), *The Principles of Geology; or, the Modern Changes of the Earth and its Inhabitants Considered as Illustrative of Geology*, vol. 3, Murray, London.

Mandelbrot, B. B. (1967), How long is the coast of Britain? Statistical self-similarity and fractal dimension, *Science*, *156*, 636–638, doi:10.1126/science.156.3775.636.

Mandelbrot, B. B. (1983), *The Fractal Geometry of Nature*, W. H. Freeman, New York.

Maritan, A., F. Colaiori, A. Flammini, M. Cieplak, and J. R. Banavar (1996), Universality classes of optimal channel networks, *Science*, *272*, 984–986, doi:10.1126/science.272.5264.984.

Niemann, J. D., R. L. Bras, D. Veneziano, and A. Rinaldo (2001), Impacts of surface elevation on the growth and scaling properties of simulated river networks, *Geomorphology*, *40*, 37–55, doi:10.1016/S0169-555X(01)00036-8.

Nozette, S., et al. (1994), The Clementine mission to the Moon: Scientific overview, *Science*, *266*, 1835–1839, doi:10.1126/science.266.5192.1835.

Price, M., and J. Suppe (1995), Constraints on the resurfacing history of Venus from the hypsometry and distribution of volcanism, tectonism, and impact craters, *Earth Moon Planets*, *50*, 25–55.

Rinaldo, A., I. Rodríguez-Iturbe, R. Rigon, E. Ijjasz-Vasquesz, and R. L. Bras (1993), Self-organized fractal river networks, *Phys. Rev. Lett.*, *70*, 822–825, doi:10.1103/PhysRevLett.70.822.

Rodríguez-Iturbe, I., and A. Rinaldo (1997), *Fractal Rivers Basins: Chance and Self-Organization*, Cambridge Univ. Press, Cambridge, U. K.

Sapoval, B., A. Baldassarri, and A. Gabrielli (2004), Self-stabilized fractality of seacoasts through damped erosion, *Phys. Rev. Lett.*, *93*, 098501, doi:10.1103/PhysRevLett.93.098501.

Smith, D. E., M. T. Zuber, G. A. Neumann, and F. G. Lemoine (1997), Topography of the Moon from the Clementine lidar, *J. Geophys. Res.*, *102*, 1591–1611, doi:10.1029/96JE02940.

Sung, Q.-C., and Y.-C. Chen (2004), Self-affinity dimensions of topography and its implications in morphotectonics: An example from Taiwan, *Geomorphology*, *62*, 181–198, doi:10.1016/j.geomorph.2004.02.012.

Turcotte, D. L. (1997), *Fractals and Chaos in Geology and Geophysics*, 2nd ed., Cambridge Univ. Press, New York.

Weissel, J. K., L. F. Pratson, and A. Malinverno (1994), The length-scaling properties of topography, *J. Geophys. Res.*, *99*, 13,997–14,012, doi:10.1029/94JB00130.

Wilson, T. H., and J. Dominic (1998), Fractal interrelationships between topography and structure, *Earth Surf. Processes Landforms*, *23*, 509–525, doi:10.1002/ (SICI)1096-9837 (199806)23:6<509::AID-ESP864>3.0.CO;2-D.

A. Baldassarri, Dipartimento di Fisica, Università di Roma "La Sapienza," Piazzale Aldo Moro 2, I-00185 Roma, Italy.

M. Montuori, CNR-INFM, Piazzale Aldo Moro 7, I-00185 Roma, Italy.

O. Prieto-Ballesteros and S. C. Manrubia, Centro de Astrobiología, CSIC-INTA, Ctra de Ajalvir km. 4, E-28850 Torrejón de Ardoz, Madrid, Spain. (cuevasms@inta.es)